International Journal of Heat and Fluid Flow 78 (2019) 108436

Contents lists available at ScienceDirect

International Journal of Heat and Fluid Flow

journal homepage: www.elsevier.com/locate/ijhff

Similarity laws for transpired turbulent flows subjected to pressure gradients, separation and wall heat transfer

M.C. Guimaraes[*,a,b], D.O.A. Cruz[a], A.P. Silva Freire[a]

[a] Programa de Engenharia Mecanica, Universidade Federal do Rio de Janeiro, Rio de Janeiro, C.P., 68503, 21945-970, Brazil

[b] Instituto Superior Técnico, Universidade de Lisboa, Lisboa 1049-001, Portugal

ARTICLE INFO

Keywords:
Similarity laws
Turbulence
Transpiration
Pressure gradient
Heat transfer

ABSTRACT

The present work proposes a new scaling and modeling procedure for the description of turbulent flows subject to wall injection or suction, non-zero pressure gradients – including flow separation – and wall heat transfer. With the proposed scaling, mean velocity and temperature profiles are self-similar with respect to the transpiration rate in the entire flow domain. All parameters appearing in the proposed expressions are shown not to vary with any of the flow variables. The near wall solutions are extended to the defect region through consideration of the intermittent character of the flow. A comparison with available experimental data shows that the intermittent factor used in this work is a universal function, independent of the transpiration rate and the pressure gradient.

1. Introduction

A problem of particular concern in the classical theory of *laminar* boundary layers is the *asymptotic suction profile*. The interest in applying distributed suction through a wall was early studied with the purpose of either preserving laminar flow under conditions which would otherwise lead to turbulent flow or maintaining flow without separation in the face of adverse pressure gradients.

In the case of a flat plate at zero incidence with uniform suction, the *laminar* boundary layer equations yield the exact solution

$$u(y) = U_\infty[1 - \exp(v_w y/\nu)]; \quad v(x, y) = v_w < 0. \tag{1}$$

Equation (1) is shown in Schlichting (1979, 7th Edition, page 385); putting $(\partial u/\partial x) \equiv 0$ into the equations of motion and $u = 0$, $v = v_w = \text{const} < 0$ for $y = 0$ and $u = U_\infty$ for $y \to \infty$, the solution follows immediately.

The resulting displacement and momentum thicknesses and wall shear stress then simply become

$$\delta_1 = \frac{\nu}{-v_w}, \quad \delta_2 = \frac{\nu}{-2v_w}, \quad \tau_w = \rho(-v_w)U_\infty. \tag{2}$$

Early experiments by Kay (1948) and Dutton (1958) demonstrated that the *laminar* exponential suction profile can be established and maintained provided the boundary layer is in an undisturbed state at the beginning of the suction region. For *turbulent* flow, the experiments also showed that an asymptotic suction profile may closely be approached at appropriate values of the suction rate. Kay further used Prandtl's mixing length theory and Taylor's vorticity transfer theory to propose two alternative forms for the mean velocity profile: a logarithmic formula and a bi-logarithmic formula.

Subsequent analyzes by Dorrance and Dore (1954), Rubesin (1954), Clarke *et al.* (1955), Dorrance (1956), van Driest (1957), Mickley and Davis (1957), Black and Sarnecki (1958), Turcotte (1960), Townsend (1961), Stevenson (1963), Marxman and Gilbert (1963), Tennekes (1964), Torii *et al.* (1966), Simpson (1967), Coles (1972) and Andersen *et al.* (1972) included transverse fluid injection at the wall and involved solutions for the mean velocity profile that presented linear (y), logarithmic ($\ln y$) or bi-logarithmic ($\ln^2 y$) terms. The studies discussed the effects of heat transfer, pressure gradients (favourable and adverse) and compressibility.

By the seventies, authors were divided as to how best represent the mean velocity profiles, through logarithmic (Tennekes, 1964; Coles, 1972; Andersen *et al.*, 1972; Watts, 1972; Afzal, 1975; Nezu, 1977) or bi-logarithmic (Clarke *et al.*, 1955; Mickley and Davis, 1957; Black and Sarnecki, 1958; Stevenson, 1963) expressions. The discussion is not simple since it involves the specification of different velocity and length scales, turbulence models, dimensional analyses and asymptotic arguments and methods. The experimental data also did not help: they did not provide conclusive evidence in favour of any particular proposition. With the passage of time, the controversy has not settled and this is clearly illustrated in the work of Vigdorovich (2016), who advocates in

* Corresponding author.
E-mail addresses: mateus_carvalho@poli.ufrj.br (M.C. Guimaraes), doac@mecanica.ufrj.br (D.O.A. Cruz).

https://doi.org/10.1016/j.ijheatfluidflow.2019.108436
Received 31 October 2018; Received in revised form 12 June 2019; Accepted 29 June 2019
Available online 14 July 2019
0142-727X/

favour of the bi-logarithmic solution.

Still, according to Vigdorovich (2016), the bi-logarithmic law is distrusted for being derived "on the basis of the Prandtl mixing-length formula, the validity of which near a permeable surface, of course, can be questioned". Actually the strongest arguments of Tennekes (1964) and Avsarkisov *et al.* (2014) against the bi-logarithmic laws relate to the adopted characteristic scales for velocity and length. In fact, the two main opposing arguments of Tennekes are that the bi-logarithmic velocity distribution does not "yield an overlap region between the wall law and the related velocity defect law and it does not include similarity of the flow in the viscous sub-layer". The comment related to the overlap region was discussed by Tennekes in terms of Millikan's analysis, which is really much less fundamental than the intermediate limit analysis of Kaplun (1967) or the matched asymptotic expansions' method. This is an elaborate discussion that will not be further pursued here. However, we notice that Silva Freire (1988b) has shown that provided adequate asymptotic expansions are specified for all flow parameters, an adequate matching can be carried out between the bi-logarithmic solutions of the viscous, defect and external flow regions.

In the present contribution, a particular decomposition of the turbulent shear stress is proposed. This decomposition splits the transport of momentum into effects associated to the turbulence of the flow and the wall transpiration. Similar procedures were recently adopted by Mendoza and Zhou (1992) and Manes *et al.* (2012). Together with a new scaling procedure (*for velocity and temperature*), the proposed expressions are capable of well representing flows subject to transpiration (blowing or suction), pressure gradients, separation and wall heat transfer. All free parameters that appear in the new expressions are shown not to vary with the transpiration rate, the pressure gradient or any other flow variable. They are thus true constants. This is in distinct contrast with some other formulations where even the constant of von Karman is subject to an empirical correction.

The near wall laws are extended to the defect layer through consideration of the intermittent character of the flow. A comparison with available experimental data shows that the intermittent factor used in this work is a universal function, independent of the transpiration rate or the pressure gradient. The complete (inner + outer) velocity and temperature mean profiles are the basis of integral methods.

The new scaling (length, velocity, temperature) for the near-wall region is appropriate for use in local analytical solutions, the numerical implementation of turbulence models or the improvement of existing turbulence models (Skote and Wallin, 2016).

The ample scope is an important aspect of the present study. Often, contributions propose isolated expressions that are shown to work for particular conditions. Most works only deal with isothermal (or adiabatic), zero-pressure gradient flows. However, results provided by bi-logarithmic laws are known to provide acceptable predictions for very complex flows. For incompressible attached flows, theoretical predictions of the friction and heat transfer coefficients are often within 3% of the experimental data (Silva Freire, 1988b; Faraco-Medeiros and Silva Freire, 1992). For compressible attached flows, predictions of the same coefficients are good to within 5% of the data (Silva Freire, 1988c; Silva Freire *et al.*, 1995). Bi-logarithmic laws are also useful in providing analytical solutions to problems that involve interaction with shock-waves (Silva Freire, 1988a) or require the specification of boundary conditions to the $\kappa - \epsilon$ model (Avelino *et al.*, 1999). Thus, it must be expected that any new proposition to the problem should be able to cover an equivalent number of applications.

Many comprehensive sets of experimental data can be found in the literature. A typical example is the thorough experimental investigation of incompressible turbulent boundary layers subject to transpiration, heat addition and adverse pressure gradients that was undertaken by the Thermosciences Division of the Mechanical Engineering Department of Stanford University. A report by Moffat and Kays (1984) summarizes the contributions of ten doctoral programs to the data base. Unfortunately, none of the data to which the present authors had access contemplated simultaneously flow transpiration, transfer of heat and separation. In fact, one experimental work was identified on transpired and separated flow. For this reason, the only comparison with experimental data presented here for transpired and separated flows uses the data of Yang *et al.* (1994).

2. Characteristic scales of the flow

For the canonical turbulent boundary layer, the celebrated velocity and length scales for the wall region are u_τ ($= \sqrt{\tau_w/\rho}$, friction velocity) and ℓ_τ ($= \nu/u_\tau$).

In the presence of wall transpiration, however, the viscous layer solution is given by

$$\frac{v_w \bar{u}}{u_\tau^2} = \exp\left(\frac{v_w y}{\nu}\right) - 1, \tag{3}$$

where $\bar{u}$ now represents the longitudinal mean velocity.

Equation (3) is shown in Tennekes (1964, page 25); it is similar to Eq. (1), but has been derived for ***turbulent*** flow by putting $u = 0$, $v = v_w = \text{const} < 0$, $\tau = \text{const} = \tau_w$ for $y = 0$.

Equation (3) suggests the similarity scales u_τ^2/v_w and ν/v_w, which cannot, of course, be used for $v_w = 0$ or even small values of the transpiration velocity. In fact, a series expansion of Eq. (3) as $v_w \to 0$ gives

$$\frac{\bar{u}}{u_\tau} = \frac{y u_\tau}{\nu} + \frac{1}{2}\frac{v_w}{u_\tau}\left(\frac{y u_\tau}{\nu}\right)^2. \tag{4}$$

In the above two term expansion, the relevant scales u_τ and ν/u_τ are recovered. The first order correction is $O(v_w/u_\tau)$ so that the approximation, Eq. (4), is valid for all boundary layers with blowing and suction in which condition $O(v_w/u_\tau) << 1$ is observed. The characteristic velocity for flows subjected to strong adverse pressure gradients and separation was shown by Goldstein (1948) to be u_p ($= ((\nu/\rho)(dP_w/dx))^{1/3}$). At a point of zero wall shear stress, successive integrations of the equations of motion give

$$\frac{\bar{u}}{u_p} = \frac{1}{2}\left(\frac{y u_p}{\nu}\right)^2. \tag{5}$$

Stratford (1959) used the mixing-length concept to find for the fully turbulent region

$$\frac{\bar{u}}{u_p} = \frac{2}{\phi\varkappa}\left(\frac{y u_p}{\nu}\right)^{1/2}, \tag{6}$$

where $\varkappa$ ($=0.4$) is the von Karman constant and ϕ ($=0.66$) is a correction to the value of $\varkappa$. This result was also derived by Stratford through dimensional analysis.

Thus, it is evident from the above that any proposed scaling procedure for flows subject to transpiration and adverse pressure gradients (with possible flow separation) needs to adjust itself to reduce to the relevant scales in the relevant limiting cases of small, moderate and large v_w and $\partial\bar{p}/\partial x$.

In particular, the structure of a turbulent boundary layer must change to accommodate the scaling of Goldstein (1948) and Stratford (1959) at a point of separation ($\bar{u}/u_p = F(y u_p/\nu)$). The DNS data of Na and Moin (1998) and Skote and Henningson (2002) confirm the existence of regions where the Goldstein's and Stratford's scaling is observed. The experimental data of Loureiro *et al.* (2007) and Loureiro and Silva Freire (2009) for flow over a smooth surface and Loureiro *et al.* (2008, 2009) for separated flow over rough surfaces also clearly show the scaling of Goldstein and Stratford at a point of $\tau_w = 0$.

To determine the characteristic scales of velocity and length (u_c, y_c) the approach of Cruz and Silva Freire (1998, 2002) is adopted here.

Consider the momentum balance in the fully turbulent region where the turbulent stresses are balanced by the local pressure gradient and the inertial term, that is,

$$v_w \frac{\partial \bar{u}}{\partial y} = -\frac{1}{\rho}\frac{\partial \bar{p}}{\partial x} - \frac{\partial}{\partial y}\overline{u'v'}. \tag{7}$$

A first integration leads to,

$$v_w \bar{u} = -\frac{1}{\rho}\frac{\partial \bar{p}}{\partial x} y - \overline{u'v'} - \frac{\tau_w}{\rho}. \tag{8}$$

Considering that the velocities scale as $\bar{u} \sim u' \sim v' \sim u_c$ and that close to the wall $y_c \sim \nu/u_c$, it results from an order of magnitude analysis of the terms in Eq. (8) (e.g., for the pressure gradient term $y\rho^{-1}\partial\bar{p}/\partial x \sim (\nu\rho^{-1}\partial\bar{p}/\partial x)/u_c = u_p^3/u_c$) and further algebraic manipulations that

$$u_c^3 - \alpha u_c^2 v_w - \tau_w u_c/\rho - (\gamma u_p)^3 = 0, \tag{9}$$

where α and γ are proportionality coefficients of order unity and τ_w and u_p satisfy the previous definitions. For later use, we define u_{cp} as the characteristic velocity scale for which $v_w = 0$, that is

$$u_{cp}^3 - \tau_w u_{cp}/\rho - (\gamma u_p)^3 = 0. \tag{10}$$

Equation (9) is an algebraic equation that can be solved for u_c, its highest real root. For boundary layer flows over an impervious surface (where $v_w = 0$) and subjected to separation, the behaviour of u_c is vastly discussed in Loureiro and Silva Freire (2011). In particular, the characteristic behaviour of u_τ, u_p and u_c is described according to the data of Na and Moin (1998) and of Loureiro *et al.* (2007). From Eq. (9), it is clear that as $v_w = 0$ and $\tau_w \to 0$, Goldstein's scaling $u_c \sim u_p$ is recovered; as $v_w = 0$ and $\partial\bar{p}/\partial x \to 0$ the friction velocity $u_c \sim u_\tau$ is obtained.

For a zero-pressure gradient flow ($\partial\bar{p}/\partial x = 0$), Eq. (9) reduces to a second-order equation with solution

$$u_c = \frac{1}{2}(\alpha v_w + \sqrt{\alpha^2 v_w^2 + 4u_\tau^2}). \tag{11}$$

For $v_w = 0$, it follows immediately that $u_c = u_\tau$. For the limiting case, $v_w/u_\tau << 1$,

$$u_c = u_\tau + \frac{1}{2}\alpha v_w + \frac{1}{8}\alpha^2 \frac{v_w^2}{u_\tau} \tag{12}$$

an expression that to the first two orders of approximation is equivalent to the one introduced by Tennekes (1964).

Equation 9 is then observed to satisfy in the limiting relevant cases all expected behaviours. An alternative scaling was introduced in Skote and Henningson (2002), whereby the viscous term is retained in the treatment of the near-wall region and the quantity y is kept as a free parameter. Note, however, that the quoted authors never considered wall transpiration in their analysis.

3. Near wall local solutions

3.1. Mean velocity profile

To find an expression for the stream-wise mean velocity profile in the near-wall fully turbulent region, consider that the behaviour of the turbulent shear stress τ_t is affected essentially by two distinct mechanisms: (i) the transport of momentum associated with the larger Reynolds-stress-carrying eddies and (ii) the injection or suction of fluid at the wall.

With this consideration, τ_t can be written as

$$\tau_t = \tau_e + \tau_{v_w}, \tag{13}$$

where the subscripts e and v_w refer respectively to eddy and wall transpiration effects.

Further, consider the eddy viscosity hypothesis

$$\tau_e = \rho u_c \ell_t \frac{\partial \bar{u}}{\partial y}, \tag{14}$$

where u_c is the characteristic velocity defined by Eq. (9) and $\ell_t = \varkappa y$ ($\varkappa = 0.4$).

An expression for the component of τ_t associated with the extra momentum transport caused by the wall transpiration (τ_{v_w}) must be related to the characteristic velocity of the flow and the injection (or suction) velocity. A simple dimensional analysis suggests

$$\tau_{v_w} = \rho\beta u_c v_w, \tag{15}$$

where β is a proportionality constant of order unity.

Equation (15) furnishes a zero contribution to the total turbulent shear stress as $v_w = 0$; positive and negative contributions follow in the case of wall injection or suction respectively. With the proposed expression for τ_{v_w}, the turbulent shear stress does not vanish at $y = 0$. The model is thus valid only in the fully turbulent region of the boundary layer. This is made clear next through an extensive analysis of many experimental data sets.

The analysis continues with the local approximate equation,

$$\begin{aligned} \tau_t &= \tau_w + \lambda\frac{dP_w}{dx}y + \rho v_w \bar{u}, \\ \rho u_c \ell_t \frac{\partial \bar{u}}{\partial y} + \rho\beta u_c v_w &= \tau_w + \lambda\frac{dP_w}{dx}y + \rho v_w \bar{u}, \end{aligned} \tag{16}$$

where λ is a dimensionless parameter.

Solutions of the above first order ordinary differential equation, Eq. (16), are not in general logarithmic solutions as demonstrated next. Only under special conditions, solutions of Eq. (16) reduce to the logarithmic law.

At the wall, the equations of motion show that the gradient of total stress normal to the wall is equal to the stream-wise pressure gradient. However, away from the wall, in the fully turbulent region, both quantities are observed to depart in view of the inertia effects. To simplify the theoretical formulation, McDonald (1969) suggested to encapsulate the inertia effects into the pressure gradient term through consideration of the parameter λ. In his work, McDonald found $\lambda = 0.7$, about the same value that was quoted by Knopp *et al.* (2015). In fact, McDonald's analysis of the data of Newman (1951) determined that the value of λ was below 0.33 as a separation point was approached. However, he concluded that $\lambda = 0.7$ is a good approximation for most of the data sets that he analysed. Perry *et al.* (1966) proposed a varying λ – 0.65 to 0.9 – while Granville (1989) set $\lambda = 0.9$. Knopp *et al.* (2015) obtained a value of $\lambda = 0.6$ for their own data and $\lambda = 0.9$ for the experiment of Skåre and Krogstad (1994).

Equation (16) can be analytically solved with Eq. (13). The solution is

$$\frac{\bar{u}}{u_c} = \frac{u_\tau^2}{u_c v_w}\left\{\left(A\frac{y u_c}{\nu}\right)^{\frac{v_w}{\varkappa u_c}} - 1\right\} + \lambda\frac{u_p^3}{\varkappa u_c^3 - u_c^2 v_w}\left(\frac{y u_c}{\nu}\right) + \beta, \tag{17}$$

where A is an integration constant.

Parameter β is obtained from the condition that Eq. (17) must contain as limiting cases the particular solutions as $v_w \to 0$ with $dP_w/dx \neq 0$ and $dP_w/dx \to 0$ with $v_w \neq 0$ (Section 3.3);

$$\beta = f(P^+) - \frac{u_\tau^2}{\varkappa u_{cp}^2}\ln(A), \tag{18}$$

where u_{cp} is the solution of Eq. (9) with $v_w = 0$ (latter justified) and $f(P^+)$ is given by (also latter justified)

$$\begin{aligned} f(P^+) = \frac{1}{2}\left(\frac{u_p}{u_{cp}}\right)^3 10.\,8^2 + \left(\frac{u_\tau}{u_{cp}}\right)^2 10.8 \\ - \left(\frac{u_\tau}{u_{cp}}\right)^2 \frac{\ln(10.8)}{\varkappa} - \lambda\left(\frac{u_p^3}{\varkappa u_{cp}^3}\right)10.8. \end{aligned} \tag{19}$$

Equation (17) exhibits four constants that need to be determined from experimental or numerical data. The values adopted in the present work are $A = 0.35$, $\alpha = 3.15$, $\lambda = 0.45$ and $\gamma = 3.4$. These constants were obtained from a large set of experimental and DNS data, that satisfied

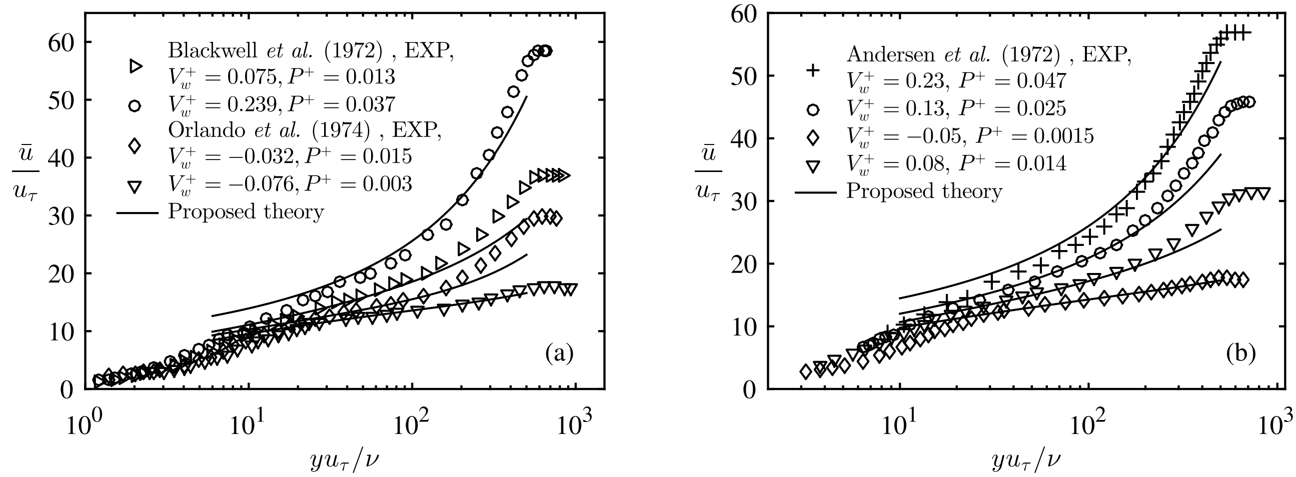

Fig. 1. Mean velocity profiles for adverse pressure gradient boundary layer flows with wall transpiration. $V_w^+ = v_w/u_\tau$; $P^+ = (u_p/u_\tau)^3$.

general as well as limiting conditions.

For example, a comparison of Eq. (17) with the results of Andersen *et al.* (1972), Blackwell *et al.* (1972) and Orlando *et al.* (1974) for turbulent boundary layer flows over flat plate walls with transpiration and mild or strong adverse pressure gradients shows that a good agreement is obtained in the near wall region (Fig. 1). A comparison of Eq. (13) with the experiments of Andersen *et al.* (1972) (Fig. 2) also shows a good agreement (in the interval $20 < yu_\tau/\nu < 250$).

The evaluation of Eq. (17) close to detachment/reattachment points (where $\tau_w \to 0$) furnishes

$$\frac{\bar{u}}{u_c} = \frac{\lambda u_p^3}{\varkappa u_c^3 - u_c^2 v_w}\left(\frac{yu_c}{\nu}\right) + \frac{10.\,8^2}{2\gamma^3} - \frac{10.8\lambda}{\varkappa\gamma^3}. \quad (20)$$

Yang *et al.* (1994) performed LDA measurements on separated-reattaching flows over a backward-facing step (BFS) with uniform normal mass injection; three non-zero injection rates were discussed. The no-injection data show that the characteristic scales proposed by Stratford (1959) furnish similarity. Wall injection, on the other hand, suggests that u_c must be the appropriate velocity scale (Fig. 3 (b)).

Equation (20) is the first scaling law presented in literature that considers the effects of wall transpiration in the regions of vanishing wall shear stress.

3.2. Mean temperature profile

The temperature law of the wall is obtained through an analogy with the fluid dynamic model.

Consider that the turbulent heat flux can be written as the sum of two components,

$$q_t = q_e + q_{v_w}, \quad (21)$$

where q_e is associated with the larger, turbulent-energy-carrying eddies and q_{v_w} represents the bulk influence of transpiration in q_t.

The first term on the right-hand side of Eq. (21), q_e, is modelled with a thermal analogy for Boussinesq's hypothesis,

$$q_e = -\rho c_p u_{cp} \ell_T \left(\frac{\tau_w + \frac{dP_w}{dx} y}{\rho u_c^2}\right)\frac{\partial \bar{T}}{\partial y}, \quad (22)$$

where $\ell_T = \varkappa_T y$ is the thermal mixing length and the factor $(\tau_w + ydP_w/dx)/\rho u_{cp}^2$ is justified in Section 3.3.2.

The remaining term is modelled through simple dimensional analysis, that is,

$$q_{v_w} = \rho c_p \tilde{\beta} v_w T_c, \quad (23)$$

where $\tilde{\beta}$ is a proportionality factor of order unity and T_c is a characteristic temperature scale given by,

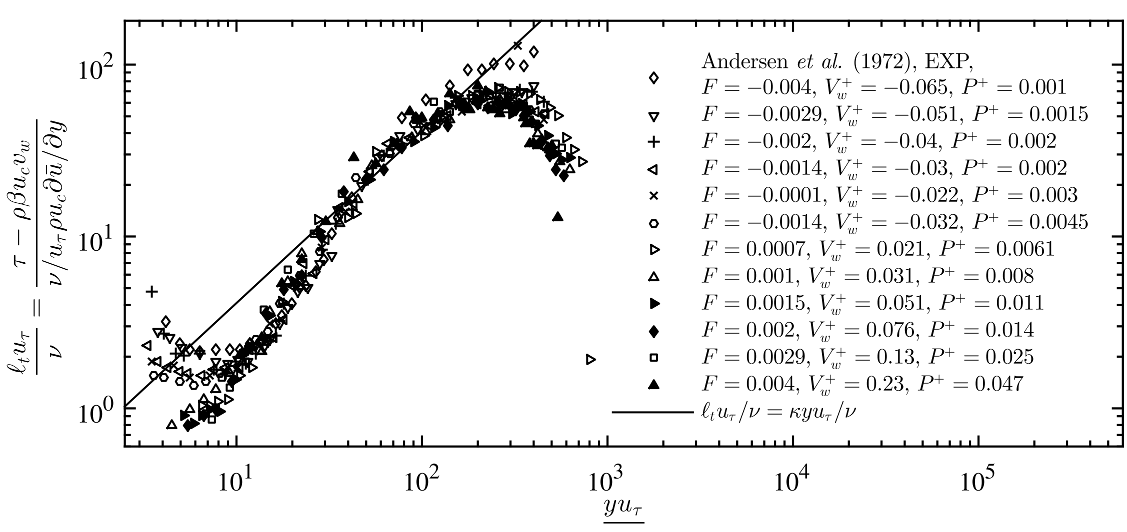

Fig. 2. Mixing length profiles for adverse pressure gradient boundary layer flows with wall transpiration accordingly to the proposed theory. $F = v_w/U_\infty$.

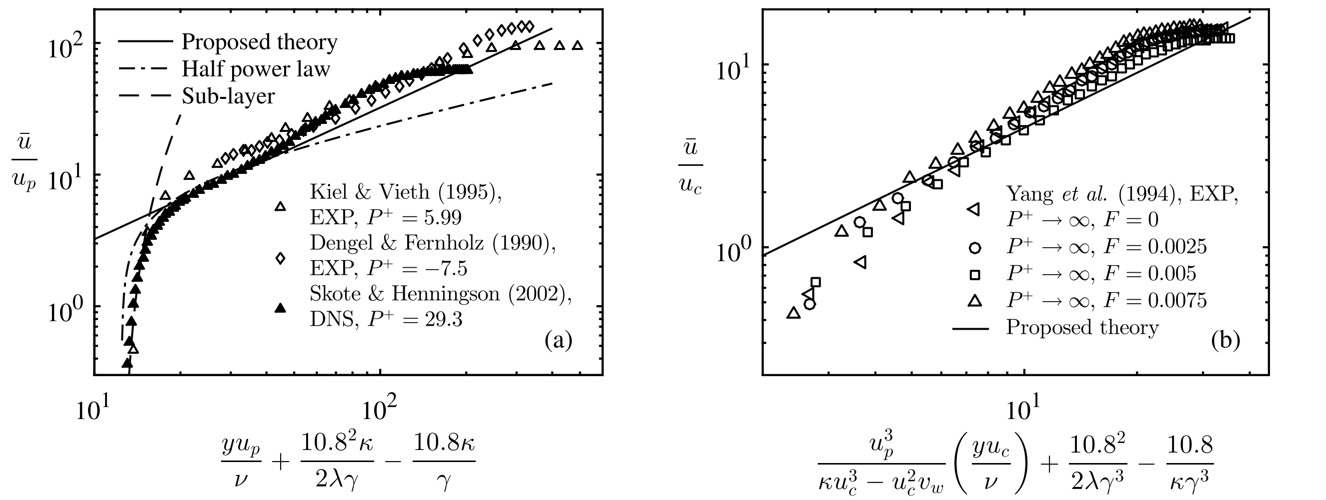

Fig. 3. Mean velocity profiles in the region of vanishing wall shear stress; (a) flat plate boundary layer non-transpired flows and (b) backward-facing step flows with wall injection.

$$T_c = \frac{q_w}{\rho c_p u_c}, \tag{24}$$

where u_c is calculated from Eq. (9) with a thermal proportionality factor ($=\gamma_T$) for the pressure gradient term.

The total turbulent heat flux is then given by

$$q_t = -\rho c_p u_c \ell_T \left(\frac{\tau_w + \frac{dP_w}{dx} y}{\rho u_{cp}^2} \right) \frac{\partial \overline{T}}{\partial y} + \tilde{\beta} \rho c_p v_w T_c. \tag{25}$$

The hypothesis, Eq. (25), is readily compared with the experimental data of Blackwell *et al.* (1972) and Orlando *et al.* (1974) in Fig. 4.

The energy equation for the near wall region is

$$q = q_w + \rho c_p v_w (T_w - \overline{T}). \tag{26}$$

A first integration, with Eq. (25), yields

$$\frac{T_w - \overline{T}}{T_c} = \frac{u_c}{v_w} \left\{ \left(\bar{C} \frac{\frac{yu_c}{\nu}}{\frac{u_\tau^2}{u_{cp}^2} + \frac{u_p^3}{u_{cp}^2 u_c} \frac{yu_c}{\nu}} \right)^{\frac{u_{cp}^2 v_w}{\varkappa_T u_c u_\tau^2}} - 1 \right\} + \tilde{\beta}. \tag{27}$$

and the constant of integration $\bar{C}$ must guarantee solution boundedness as $u_\tau \to 0$ with $v_w \neq 0$ and the correct asymptotic behaviours as $dP_w/dx \to 0$ with $v_w \neq 0$ and $v_w \to 0$ with $dP_w/dx \neq 0$ (Section 3.3).

The simplest possible proposition is

$$\bar{C} = A_T^{u_\tau^2/u_{cp}^2} \gamma_T^{3(u_\tau^3/u_{cp}^3 - 1)}. \tag{28}$$

The new temperature law of the wall, Eq. (27), exhibits three constants that need to be determined from experimental data ($\tilde{\beta}$ is evaluated from Eq. (33)). The values adopted in the present work are $\gamma_T = 3.1$, $A_T = 0.6$ and $\alpha = 3.15$.

Equation (27) is tested against the experimental data of Blackwell *et al.* (1972) and Orlando *et al.* (1974) for strong and mild APG boundary layers with wall injection and suction in Fig. 5. Equation (27) furnishes a good fit to the data except for the higher injection rate.

Equation (27) in regions of vanishing wall shear stress, reduces to

$$\frac{T_w - \overline{T}}{T_c} = \frac{u_c}{v_w} \left\{ \left[\exp\left(1 - \gamma_T^3 \frac{\nu}{yu_c} + \ln A_T \right) \right]^{\frac{v_w}{\varkappa_T u_c}} - 1 \right\} + \tilde{\beta}. \tag{29}$$

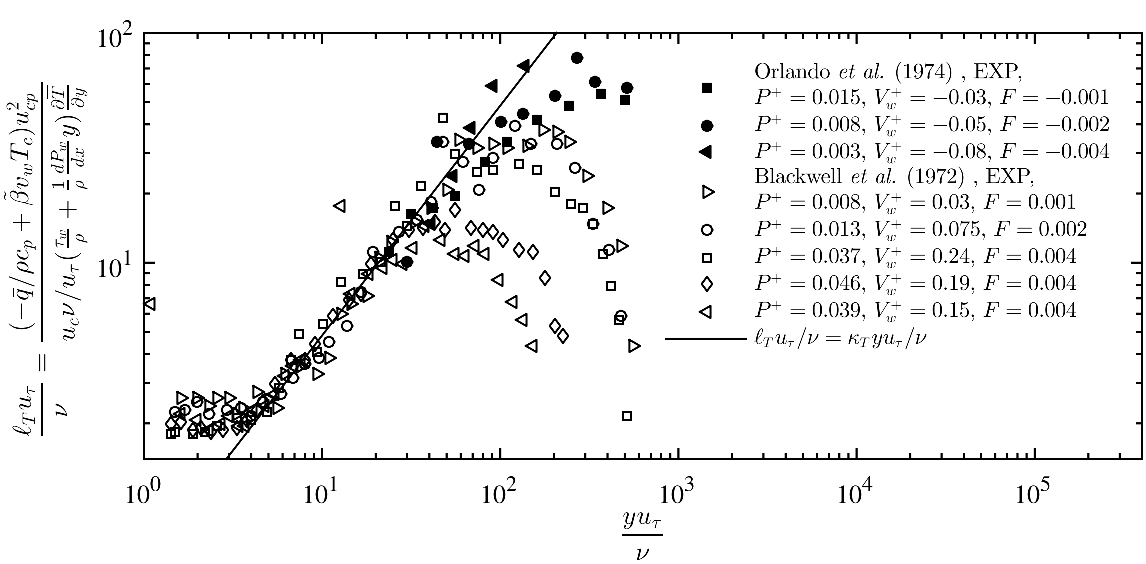

Fig. 4. Temperature mixing-length profiles for adverse pressure gradient boundary layer flows with wall transpiration.

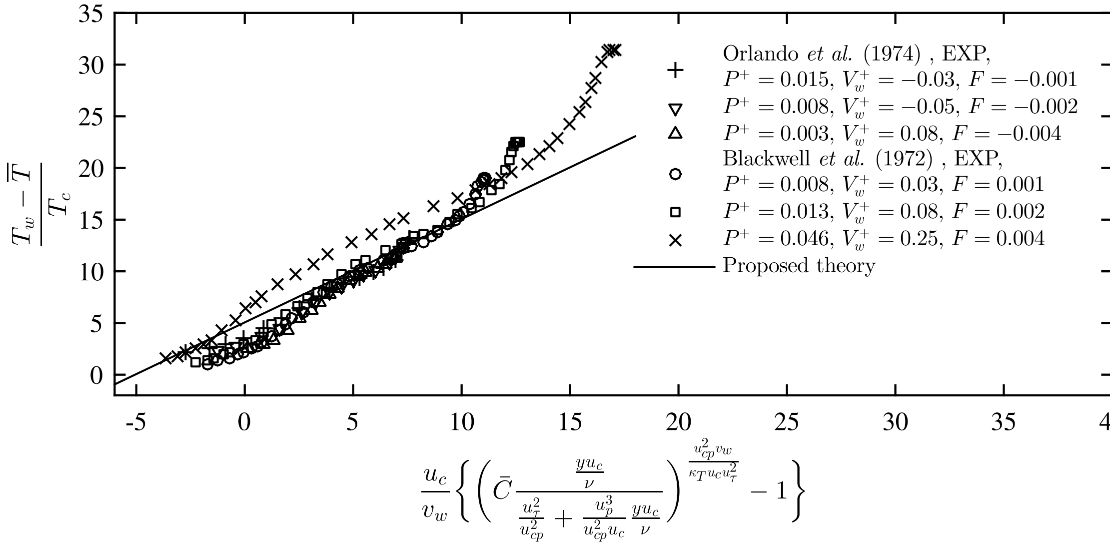

Fig. 5. Mean temperature profiles for adverse pressure gradient boundary layer flows with wall transpiration.

3.3. Limiting cases

3.3.1. Zero-pressure gradient flows with wall injection or suction

In the particular case $dP_w/dx = 0$ and $v_w \neq 0$, Eq. (17) reduces to

$$\frac{\bar{u}}{u_c} = \frac{u_\tau^2}{u_c v_w}\left\{\left(A\frac{yu_c}{\nu}\right)^{\frac{v_w}{\varkappa u_c}} - 1\right\} + \beta. \tag{30}$$

Clearly, the classical logarithmic-law of the wall is recovered as $v_w \to 0$ provided

$$\beta = 5 - \frac{1}{\varkappa}\ln(A). \tag{31}$$

Equation (30) is compared in Fig. 6 with the boundary layer data of Andersen *et al.* (1972), Baker and Launder (1974), Kornilov and Boiko (2014, 2016) for injection, Simpson (1967), Trip and Fransson (2014), Bobke *et al.* (2016), Ferro *et al.* (2017) and Khapko *et al.* (2016) for suction, the pipe flow with suction of Elena (1977) and the closed channel flows with wall injection of Nikitin and Pavel'ev (1998), Sumitani and Kasagi (1995) and Avsarkisov *et al.* (2014).

The values of the calibration constants are $A = 0.35$ and $\alpha = 3.15$. The excellent collapse of the profiles suggests that self-similarity with respect to the transpiration velocity is captured.

The mixing-length hypothesis advanced by Eq. (13) is corroborated in Fig. 7.

The temperature profile, Eq. (27), becomes

$$\frac{T_w - \overline{T}}{T_c} = \frac{u_c}{v_w}\left\{\left(A_T\frac{yu_c}{\nu}\right)^{\frac{v_w}{\varkappa_T u_c}} - 1\right\} + \tilde{\beta}, \tag{32}$$

where A_T is a constant of integration.

The numerical value of $\tilde{\beta}$ is obtained as Eq. (32) is considered in the limit $v_w \to 0$, that is,

$$\tilde{\beta} = C(Pr) - \frac{1}{\varkappa_T}\ln(A_T), \tag{33}$$

and $C(Pr)$ is the y-axis intercept of the temperature logarithmic law for non-transpired flows (Pr is the molecular Prandtl number).

Mean temperature profiles for flows with various transpiration rates are shown in Fig. 8 according to the injection and suction data of Whitten (1967) and Sumitani and Kasagi (1995). A curve fit to the temperature profiles furnishes $A_T = 0.6$ and $\alpha = 3.15$.

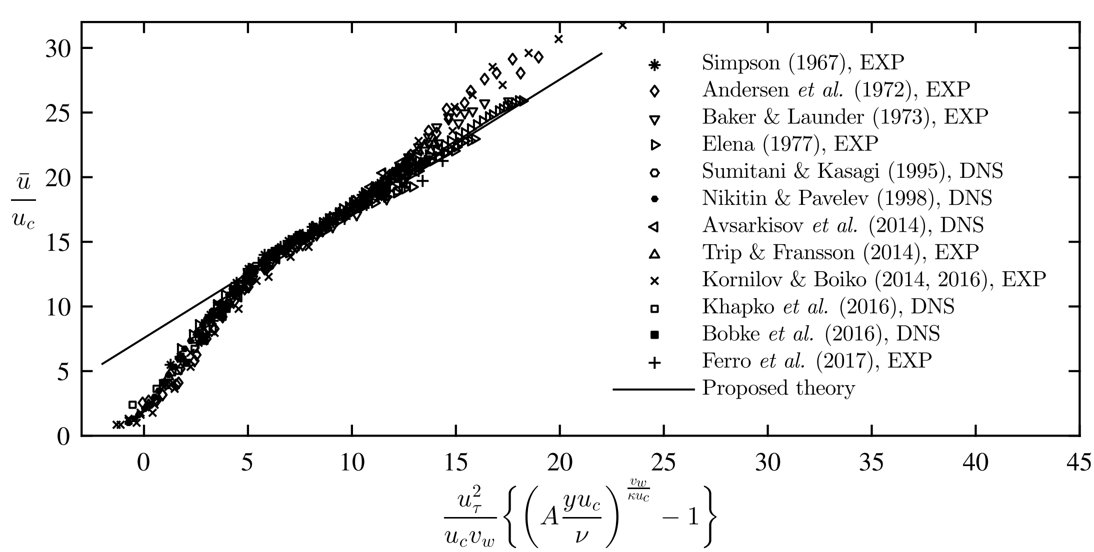

Fig. 6. Thirty two mean velocity profiles for zero-pressure-gradient (ZPG) transpired flows shown in similarity coordinates. The values of the transpiration parameters are in the range $-0.00345 \leq F \leq 0.0164$, $-0.065 \leq V_w^+ \leq 0.87$.

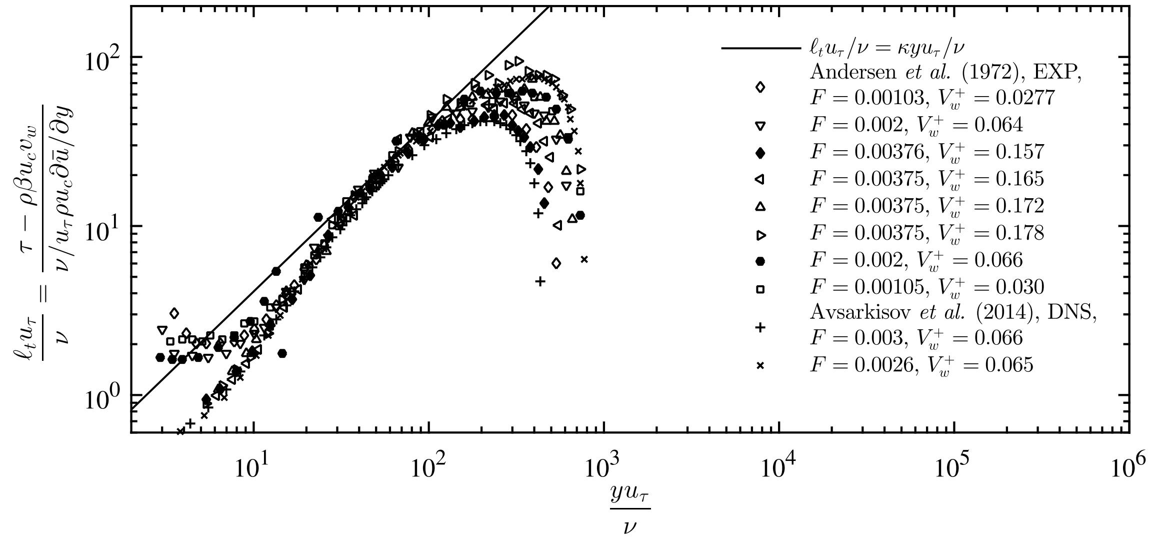

Fig. 7. Mixing-length profiles for ZPG flows with wall transpiration.

The validity of the mixing length hypothesis is tested against the DNS data of Sumitani and Kasagi (1995) in Fig. 9 with $\tilde{\beta}$ obtained from Eq. (33).

3.3.2. Variable pressure gradient flows with no injection or suction

Equation (17) under the conditions $v_w \to 0$ and $dP_w/dx \neq 0$ reduces to

$$\frac{\bar{u}}{u_c} = \frac{u_\tau^2}{\varkappa u_c^2}\ln\left(\frac{y u_c}{\nu}\right) + \lambda\frac{u_p^3}{\varkappa u_c^3}\left(\frac{y u_c}{\nu}\right) + f(P^+), \tag{34}$$

where $f(P^+)$ is a constant of integration (in yu_c/ν).

Equation (34) is similar to previous formulations of other authors (Simpson, 1983; Wilcox, 1989); in particular, it contains a combination of logarithmic and linear terms. As experimental and DNS mean velocity data are shown in coordinates yu_c/ν and u/u_c, they appear to exhibit a straight line behavior in a well-defined region but do not collapse onto a single curve. The conclusion is that f is indeed a function of P^+.

To determine $f(P^+)$, use is made of the intercept between the sublayer and the fully turbulent solutions, the point (y_a, u_a). In the viscous sub-layer solution,

$$\frac{\bar{u}}{u_\tau} = \frac{y u_\tau}{\nu} + \frac{1}{2}\left(\frac{u_p}{u_\tau}\right)^3\left(\frac{y u_\tau}{\nu}\right)^2, \tag{35}$$

an equation that can be used to express u_a in terms of y_a.

In the limit $dP_w/dx \to 0$, $y_a u_\tau/\nu$ is 10.8. A generalization of this result is

$$\frac{y_a u_c}{\nu} = 10.8, \tag{36}$$

from which Eq. (19) follows.

Figure 10 compares Eq. (34) ($\lambda = 0.45$ and $\gamma = 3.4$) with the data of Kiel (1995), Marusic and Perry (1995), Na and Moin (1998), Bernard *et al.* (2003), Willert (2015) and Gungor *et al.* (2016).

Many authors consider the mixing-length a rather restrictive postulate, in particular, for flows subjected to adverse pressure gradients. The data of Marusic and Perry (1995), Dengel and Fernholz (1990), Skote and Henningson (2002), and Gungor *et al.* (2016) show that application of the mixing-length theory does not conflict with experiments (Fig. 11).

Near to a separation or reattachment point, Eq. (34) takes on the form

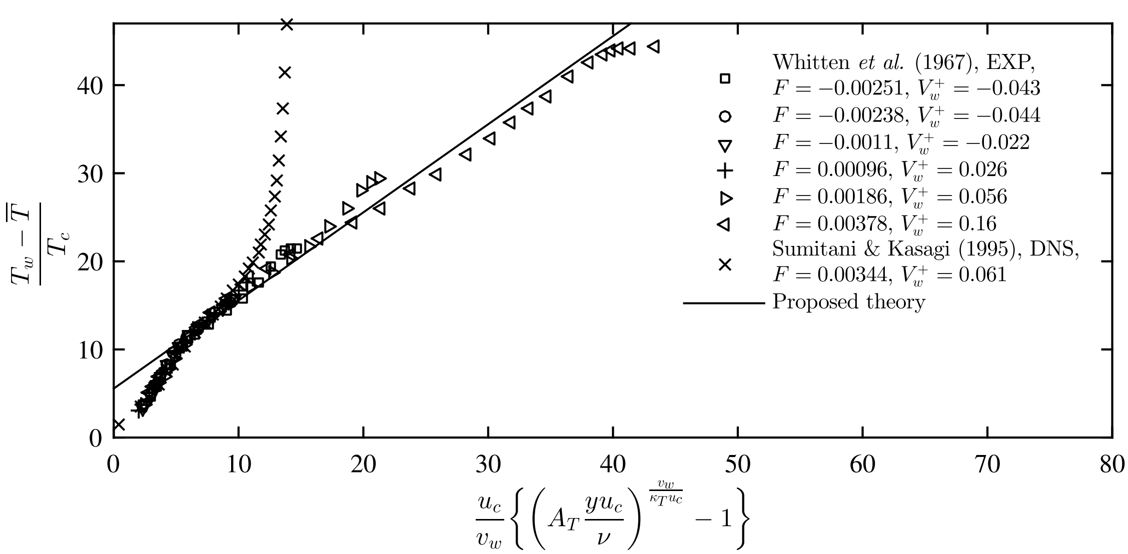

Fig. 8. Mean temperature profiles for ZPG transpired flows shown in similarity coordinates.

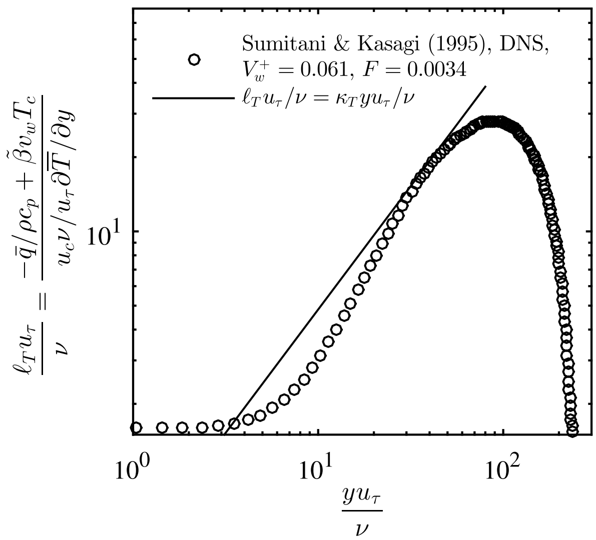

Fig. 9. Temperature mixing-length profile for channel flow with wall transpiration.

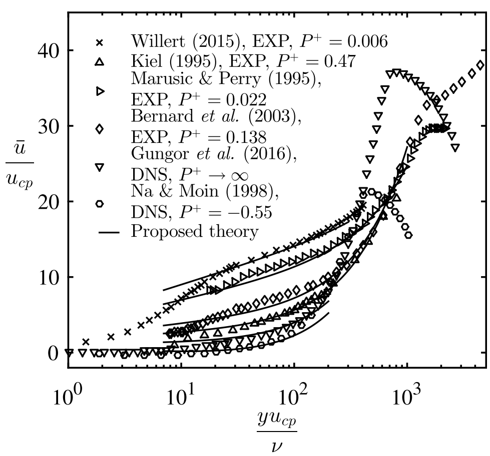

Fig. 10. Mean velocity profiles for adverse pressure gradient boundary layer flows.

$$\frac{\bar{u}}{u_p} = \frac{\lambda}{\varkappa\gamma}\left(\frac{yu_p}{\nu}\right) + \frac{10.\,8^2}{2\gamma^2} - \frac{10.8\lambda}{\varkappa\gamma^2}. \tag{37}$$

This result is different from Stratford's half power law. However, when mean velocity profiles are shown in a non-dimensional linear coordinates system, a linear portion in the near wall region can be identified (Fig. 3 (a), Stratford's half power law is also shown for comparison).

The experimental data of Blackwell *et al.* (1972) and Pak (1999) suggest that the turbulent Prandtl number near the wall is a function of the pressure gradient parameter. In an alternative approach to the use of the turbulent Prandtl number concept, a new closure expression for the turbulent flux of heat q_t $(=\rho c_p \overline{v'T'})$ based on simple order of magnitude considerations and the mixing length model can be summoned. Consider $v' \sim \sqrt{\overline{u'v'}} = \sqrt{\varkappa y u_c \partial\bar{u}/\partial y} = \sqrt{\tau_w/\rho + (y/\rho)dP_w/dx}$, where the identities stem from the mixing-length theory for the transfer of mean momentum. Equivalently, consider for the temperature fluctuation, $T' \sim \sqrt{-\varkappa_T y T_c \partial\overline{T}/\partial y}$, so that q_t can be cast as

$$q_t = \rho c_p \sqrt{\frac{\tau_w}{\rho} + \frac{1}{\rho}\frac{dP_w}{dx}y}\ \sqrt{-\varkappa_T y T_c \frac{\partial\overline{T}}{\partial y}}. \tag{38}$$

Integration of Eq. (38) together with the energy equation ($q_t = q_w$) leads to

$$\frac{T_w - \overline{T}}{T_c} = \frac{1}{\varkappa_T}\frac{u_c^2}{u_\tau^2}\left\{\ln\left(\frac{yu_c}{\nu}\right) - \ln\left(\frac{u_\tau^2}{u_c^2} + \frac{u_p^3}{u_c^3}\frac{yu_c}{\nu}\right)\right\} + \tilde{C}, \tag{39}$$

where $\tilde{C}$ must be determined so as to guarantee solution boundedness as $u_\tau \to 0$ and the correct asymptotic behaviour as $dP_w/dx \to 0$, that is,

$$\tilde{C} = \frac{1}{\varkappa_T}\frac{u_c^2}{u_\tau^2}\ln(\gamma_T^{-3}) - \frac{1}{\varkappa_T}\frac{u_\tau}{u_c}\ln(\gamma_T^{-3}) + C(Pr), \tag{40}$$

where $C(Pr)$ is the intercept of the temperature solution for zero pressure gradient flows. Since $u_p^3/u_c^3 \to \gamma_T^{-3}$ as $u_\tau \to 0$, the first term on the r.h.s. of Eq. (40) assures boundedness in that limit; since $u_c/u_\tau \to 1$ as $dP_w/dx \to 0$ the last two terms make the solution correct for zero pressure gradient flows.

The temperature solution can then be written as

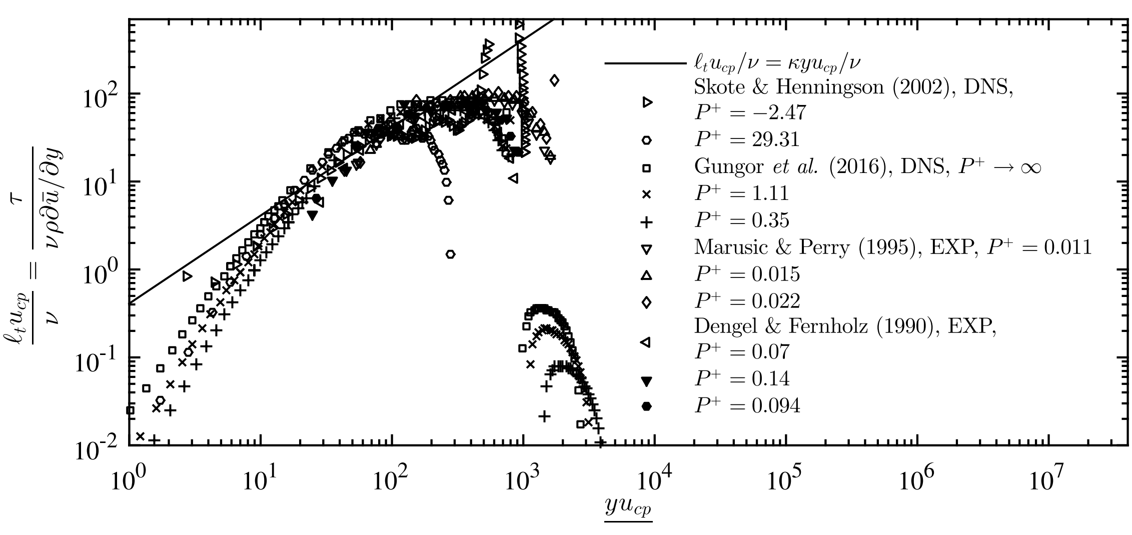

Fig. 11. Mixing-length profiles for adverse pressure gradient boundary layer flows.

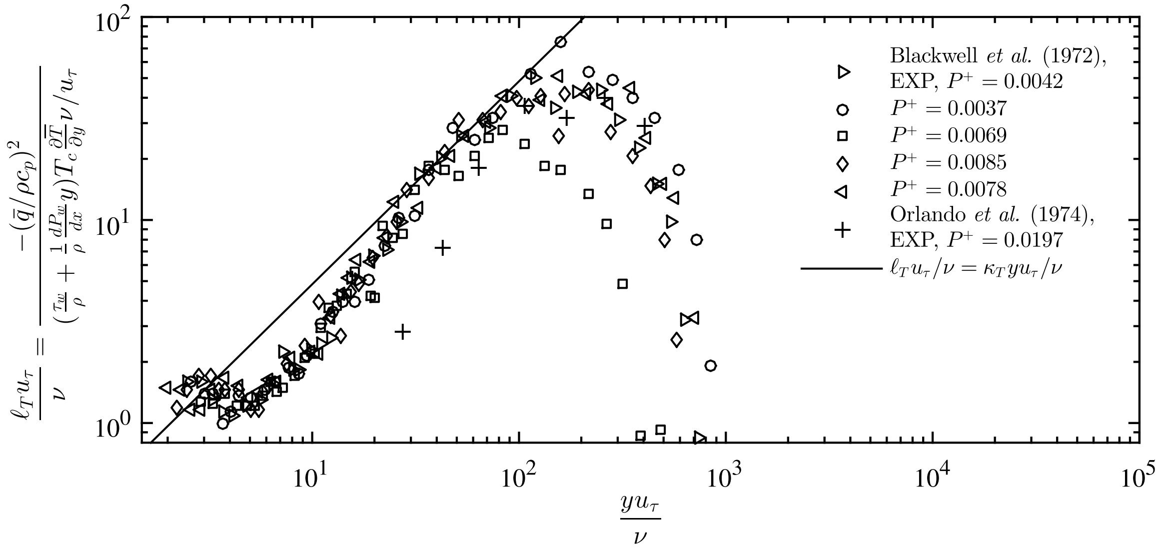

Fig. 12. Temperature mixing-length profiles for adverse pressure gradient boundary layer flows.

$$\frac{T_w-\overline{T}}{T_c} = \frac{1}{\varkappa_T}\ln\left\{\frac{\left(\frac{yu_c}{\nu}\gamma_T^{-3}\right)^{\frac{u_c^2}{u_\tau^2}}\gamma_T^{\frac{3u_\tau}{u_c}}}{\left(\frac{u_\tau^2}{u_c^2}+\frac{u_p^3}{u_c^3}\frac{yu_c}{\nu}\right)^{\frac{u_c^2}{u_\tau^2}}}\right\} + C(Pr), \tag{41}$$

Figure 13 (a) shows the data of Blackwell *et al.* (1972) and Orlando *et al.* (1974) in comparison with Eq. (41). The thermal mixing length hypothesis is corroborated in Fig. 12.

In the region of vanishing wall shear stress Eq. (41) reduces to an inverse linear power law,

$$\frac{T_w-\overline{T}}{T_p} = -\frac{\gamma_T}{\varkappa_T}\left(\frac{yu_p}{\nu}\right)^{-1} + \frac{C(Pr)}{\gamma_T} + \frac{1}{\gamma_T\varkappa_T}. \tag{42}$$

A comparison between the data of Vogel (1984) for flow over a backward-facing step, and Eq. (42) in Fig. 13(b) furnishes a good agreement.

In Section 3.2 the equation for q_e, Eq. (22), was introduced so as to guarantee the correct asymptotic behaviour of q_t and $\overline{T}$ as the limit cases are considered.

4. Defect layer solution

To extend the near wall solutions to the defect region of turbulent boundary layers, the intermittent character of turbulence is used.

All turbulent flows with a free boundary exhibit a distinctly sharp and very thin region that varies continuously with position and time and separates regions of turbulent (T) and non-turbulent (NT) flow (Klebanoff, 1955; Corrsin and Kistler, 1955). The T/NT interface is normally referred to as the viscous superlayer and is shown – depending on the flow nature – to have its thickness scaled with the Kolmogorov length, Taylor's micro-scale or the friction length. An excellent review on interface layers is found in da Silva *et al.* (2014).

The intermittency hypothesis of Sarnecki (1959) postulates that the mean velocity profile in the outer region of a turbulent boundary layer can be represented through,

$$\bar{u} = \gamma_s u_{\text{turb}} + (1-\gamma_s)u_{\text{pot}}, \tag{43}$$

where u_{turb} and u_{pot} are respectively the mean velocities whether the flow is turbulent or potential (or non-turbulent). Sarnecki further considers that $u_{\text{pot}} = U_\infty$ and u_{turb} is obtained from the near wall solution. These considerations imply that there is a discontinuous velocity jump

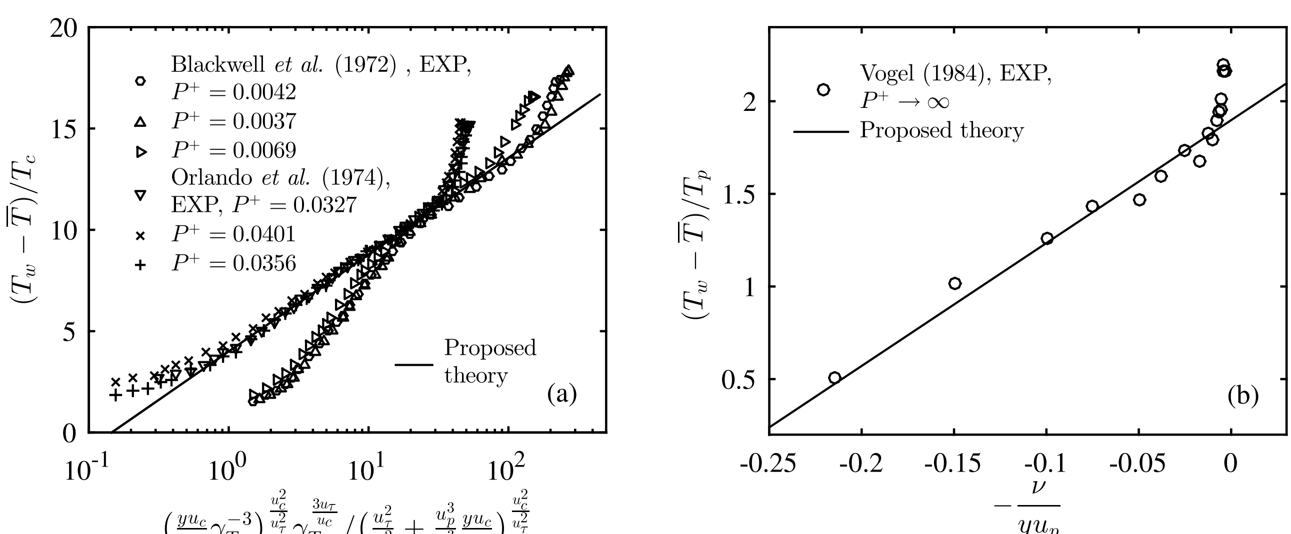

Fig. 13. Mean temperature profiles for adverse pressure gradient flows; (a) flat plate boundary layer and (b) backward-facing step at the reattachment point.

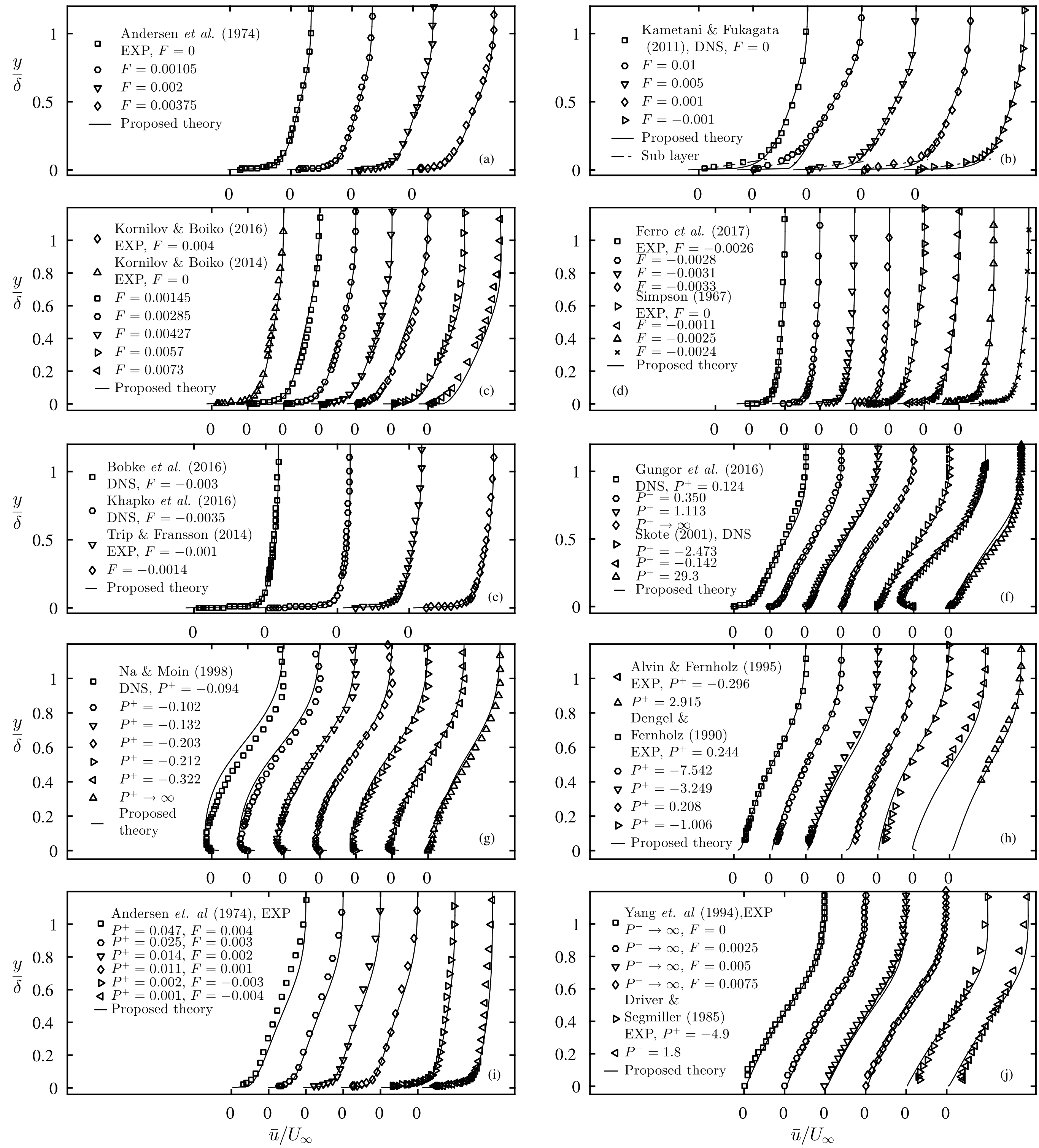

Fig. 14. Mean velocity profiles shown in outer coordinates; (a-c) ZPG flows with wall injection, (d-e) ZPG flows with wall suction, (f-h) strong APG and separated non-transpired flows, (i) APG flows with wall injection or suction and (j) backward-facing step flows with wall injection.

at the interface. However, since the thickness of the superlayer is very thin compared to the flow width, all field variables vary smoothly across the boundary layer.

The intermittent factor (γ_s) is given by the error function,

$$\gamma_s(y/\delta) = \frac{1}{2}\left[1 - \operatorname{erf}\left(\frac{y/\delta - \mu/\delta}{\sqrt{2}\,\sigma/\delta}\right)\right], \tag{44}$$

where the boundary layer thickness δ is defined by $\bar{u}(x, y = \delta) = 0.99U_\infty$. Experimental data reveal that parameters μ/δ and σ/δ do not vary with the transpiration velocity or the pressure gradient parameter and γ_s is a universal function of y/δ. Parameters μ and σ are the mean and standard deviation in a Gaussian distribution of $Y(t)$, the position of the turbulent/non-turbulent (T/NT) interface. Appropriate values are $\mu/\delta = 0.78$ and $\sigma/\delta = 0.14$ (Klebanoff, 1955) and $\mu/\delta = 0.66$ and $\sigma/\delta = 0.11$ (Chauhan *et al.*, 2014).

In Fig. 14 all profiles are shown with $\mu/\delta = 0.66$ and $\sigma/\delta = 0.23$. The

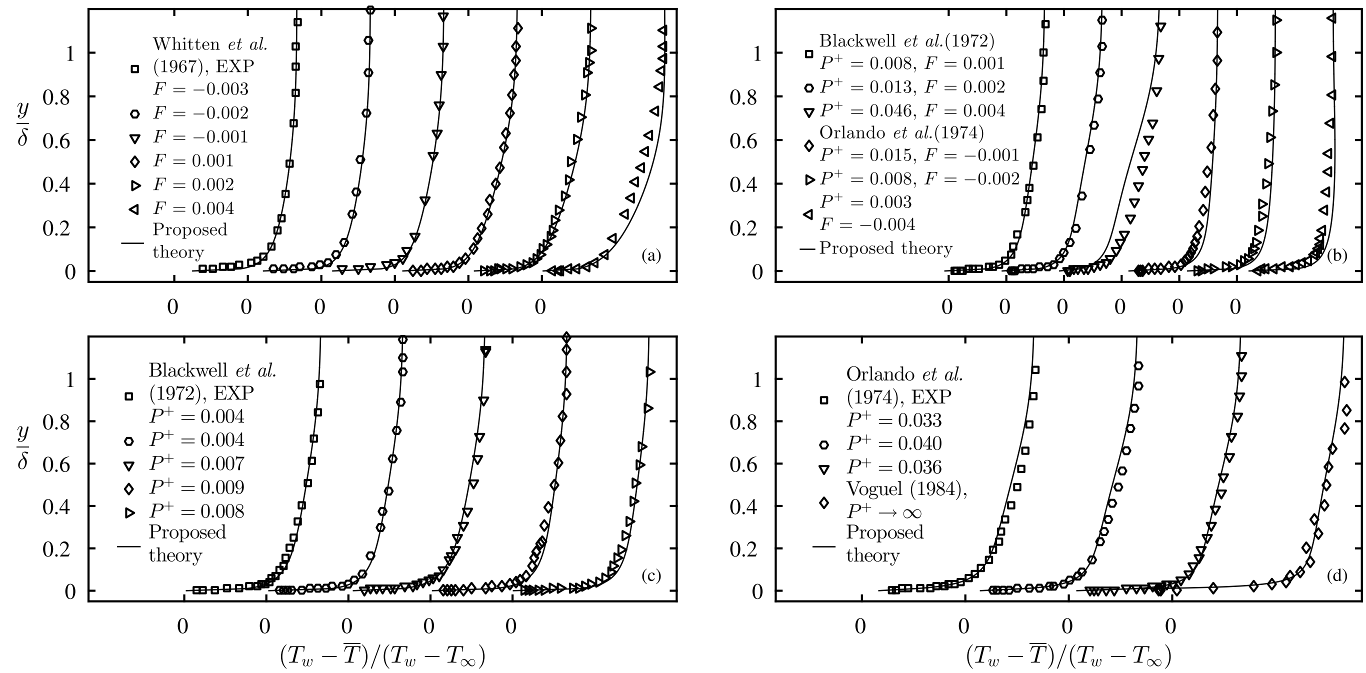

Fig. 15. Mean temperature profiles shown in outer coordinates; (a) ZPG flows with wall injection or suction, (b) APG flows with wall injection or suction, (c-d) APG and separated non-transpired flows.

expressions provide an excellent fit to the data throughout the flow field, including the near wall region ($y/\delta < 0.1$ approximately). Profiles in regions of reverse flow are known to be particularly difficult to predict, in particular in the small portion where $\bar{u}$ is negative. The present approach, however, is noted to furnish good predictions. In the particular case of a flow with $v_w = 0$ and $\partial\bar{p}/\partial x = 0$ the intermittency hypothesis of Sarnecki (1959) coincides with the two-state model proposed by Krug *et al.* (2017).

In the defect region, an expression for the mean temperature profile is proposed based on a straight analogy with the velocity case. Consider that the temperature difference $T_w - \overline{T}$ can be expressed by the following equation,

$$T_w - \overline{T} = \varphi(T_w - T_{\text{turb}}) + (1 - \varphi)(T_w - T_\infty), \tag{45}$$

where $T_w - T_{\text{turb}}$ is obtained from the near wall solution and φ is the thermal intermittent factor.

Equation (45) is refereed to as the *thermal intermittency hypothesis*. φ is given by

$$\varphi(y/\delta) = \frac{1}{2}\left[1 - \text{erf}\left(\frac{y/\delta - \mu_T/\delta}{\sqrt{2}\,\sigma_T/\delta}\right)\right], \tag{46}$$

where μ_T and σ_T are analogous to μ and σ but are associated with the transfer of heat.

The temperature intermittent hypothesis must represent the scalar gradient T/NT interface as made clear by Silva and da Silva (2017).

Figure 15 shows comparisons between mean temperature profiles obtained through the temperature intermittent hypothesis (with $\mu_T = 0.6$ and $\sigma_T = 0.3$) and the experimental data of Whitten (1967), Blackwell *et al.* (1972), Orlando *et al.* (1974) and Vogel (1984). The excellent agreement between theory and the data shows that φ is a universal function of y/δ; thus, φ does not depend on the transpiration rate, the pressure gradient parameter or the Reynolds number.

5. Final remarks

The present work has proposed some new scaling laws for transpired turbulent flows with non-zero pressure gradients and wall heat transfer. With the proposed scaling, mean velocity and temperature profiles are self-similar with respect to the transpiration rate in the entire flow domain.

In the proposed formulation, all free parameters are constants that do not vary with the transpiration rate or the pressure gradient parameter. The intermittent character of turbulence was used to extend the domain of validity of the near wall solutions to the outer region of the domain. The *intermittent factor* is found to be a universal function of the wall normal direction scaled by the boundary layer thickness.

Acknowledgments

APSF is grateful to the Brazilian National Research Council (CNPq) for the award of a Research Fellowship (No. 305338/2014-5). The work was financially supported by the Rio de Janeiro Research Foundation (FAPERJ) through Grant E-26/202.912/2015. MCG is grateful to Professors Ayse Gungor and Martin Skote for providing their DNS data, Juliana Loureiro and Yvan Maciel for their experimental data, Doug McLean, George Mellor, Hiroyuki Abe, Jens Fransson, John Eaton, Klaus Gersten, Marco Ferro, Martin Oberlack, Roney Thompson, Uzak Zhapbasbayev and the U.S. Defense Technical Information Center Reference team for the many publications sent to the author when requested. MCG particularly thanks Prof. Carlos da Silva of the IST/Portugal for some interesting suggestions.

References

Afzal, N., 1975. Effects of longitudinal curvature, vorticity and displacement for two-dimensional turbulent boundary layers with heat and mass transfer. J. Mécanique 14 (5).

Andersen, P.S., Kays, W.M., Moffat, R.J., 1972. The turbulent boundary layer on a porous plate: an experimental study of the fluid mechanics for adverse free-stream pressure gradients. In: Report HMT-15. Stanford University.

Avelino, M.R., Su, J., Silva Freire, A.P., 1999. An analytical near wall solution for the κ–ϵ model for transpired boundary layer flows. Int. J. Heat Mass Transfer 42 (16), 3085–3096.

Avsarkisov, V., Oberlack, M., Hoyas, S., 2014. New scaling laws for turbulent poiseuille flow with wall transpiration. J. Fluid Mech. 746, 99–122.

Baker, R., Launder, B.E., 1974. The turbulent boundary layer with foreign gas injection-I. Measurements in zero pressure gradient. Int. J. Heat Mass Transfer 17 (2), 275–291.

Bernard, A., Foucaut, J., Dupont, P., Stanislas, M., 2003. Decelerating boundary layer: a new scaling and mixing length model. AIAA J. 41 (2), 248–255.

Black, T., Sarnecki, A., 1958. The Turbulent Boundary Layer with Suction Or Injection.

Reports and Memoranda 3387. Aeronautical Research Council.
Blackwell, B.F., Kays, W.M., Moffat, R.J., 1972. The turbulent boundary layer on a porous plate: an experimental study of the heat transfer behavior with adverse pressure gradients. Report HMT-16. NASA, Stanford University.
Bobke, A., Örlü, A., Schlatter, P., 2016. Simulations of turbulent asymptotic suction boundary layers. J. Turbul. 17 (2), 157–180.
Chauhan, K., Philip, J., Marusic, I., 2014. Scaling of the turbulent/non-turbulent interface in boundary layers. J. Fluid Mech. 751, 298–328.
Clarke, J.H., Menkes, H.R., Libby, P.A., 1955. A provisional analysis of turbulent boundary layers with injection. J. Aeronaut. Sci. 22 (4), 255–260.
Coles, D., 1972. A survey of data for turbulent boundary layers with mass transfer. Proceedings of the AGARD Conference on Turbulent Shear Flows, London.
Corrsin, S., Kistler, A.L., 1955. Free-stream boundaries of turbulent flows. Technical Report 1244. National Advisory Committee for Aeronautics.
Cruz, D.O.A., Silva Freire, A.P., 1998. On single limits and the asymptotic behaviour of separating turbulent boundary layers. Int. J. Heat Mass Transfer 41 (14), 2097–2111.
Cruz, D.O.A., Silva Freire, A.P., 2002. Note on a thermal law of the wall for separating and recirculating flows. Int. J. Heat Mass Transfer 45 (7), 1459–1465.
Dengel, P., Fernholz, H.H., 1990. An experimental investigation of an incompressible turbulent boundary layer in the vicinity of separation. J. Fluid Mech. 212, 615–636.
Dorrance, W.H., 1956. The effect of mass transfer on the compressible turbulent boundary-layer skin friction and heat transfer—an addendum. J. Aeronaut. Sci. 23 (3), 272–288.
Dorrance, W.H., Dore, F.J., 1954. The effect of mass transfer on the compressible turbulent boundary-layer skin friction and heat transfer. J. Aeronaut. Sci. 21 (6), 404–410.
van Driest, E.R., 1957. On Mass Transfer near the Stagnation Point. Technical Notes 57–458. Air Force Office of Scientific Research.
Dutton, R.A., 1958. The Effects of Distributed Suction on the Development of Turbulent Boundary Layers. Reports and Memoranda 3155. Aeronautical Research Council.
Elena, M., 1977. Study of the dynamic and thermal fields in a turbulent pipe flow with wall suction. Technical Report. France, CEA-R–4843
Faraco-Medeiros, M.A., Silva Freire, A.P., 1992. The transfer of heat in turbulent boundary layers with injection or suction: universal laws and Stanton number equations. Int. J. Heat Mass Transfer 35 (4), 991–995.
Ferro, M., Fallenius, B.E.G., Fransson, J.H.M., 2017. On the scaling of turbulent asymptotic suction boundary layers. 10th International Symposium on Turbulence and Shear Flow Phenomena (TSFP10). Chicago, USA
Goldstein, S., 1948. On laminar boundary-layer flow near a position of separation. Q. J. Mech. Appl.Math. 1 (1), 43–69.
Granville, P.S., 1989. A modified van Driest formula for the mixing length of turbulent boundary layers in pressure gradients. J. Fluids Eng. 111 (1), 94–97.
Gungor, A.G., Maciel, Y., Simens, M.P., Soria, J., 2016. Scaling and statistics of large-defect adverse pressure gradient turbulent boundary layers. Int. J. Heat Fluid Flow 59, 109–124.
Kaplun, S., 1967. Fluid Mechanics and Singular Perturbations. Academic Press, New York.
Kay, J.M., 1948. Boundary-Layer Flow along a flat Plate with Uniform Suction. Reports and Memoranda 2628. Aeronautical Research Council.
Khapko, T., Schlatter, P., Duguet, Y., Henningson, D.S., 2016. Turbulence collapse in a suction boundary layer. J. Fluid Mech. 795, 356–379.
Kiel, R., 1995. Experimentelle Untersuchung einer Strömung mit beheiztem lokalen Ablösewirbel an einer geraden Wand. VDI-Verlag.
Klebanoff, P.S., 1955. Characteristics of turbulence in boundary layer with zero pressure gradient. Technical Report 1247. National Advisory Committee for Aeronautics.
Knopp, T., Buchmann, N.A., Schanz, D., Eisfeld, B., Cierpka, C., Hain, R., Schröder, A., Kähler, C., 2015. Investigation of scaling laws in a turbulent boundary layer flow with adverse pressure gradient using PIV. J. Turbul. 16 (3), 250–272.
Kornilov, V.I., Boiko, A.V., 2014. Formation of the turbulent boundary layer at air blowing through a wall with an abrupt change in boundary conditions. Thermophys. Aeromech. 21 (4), 421–439.
Kornilov, V.I., Boiko, A.V., 2016. Experimental modeling of air blowing into a turbulent boundary layer using an external pressure flow. Tech. Phys. 61 (10), 1480–1488.
Krug, D., Philip, J., Marusic, I., 2017. Revisiting the law of the wake in wall turbulence. J. Fluid Mech. 811, 421–435.
Loureiro, J.B.R., Monteiro, A.S., Pinho, F.T., Silva Freire, A.P., 2008. Water-tank studies of separating flow over rough hills. Boundary Layer Meteorol. 129 (2), 289.
Loureiro, J.B.R., Monteiro, A.S., Pinho, F.T., Silva Freire, A.P., 2009. The effect of roughness on separating flow over two-dimensional hills. Exp. Fluids 46 (4), 577.
Loureiro, J.B.R., Pinho, F.T., Silva Freire, A.P., 2007. Near wall characterization of the flow over a two-dimensional steep smooth hill. Exp. Fluids 42 (3), 441–457.
Loureiro, J.B.R., Silva Freire, A.P., 2009. Note on a parametric relation for separating flow over a rough hill. Boundary Layer Meteorol. 131 (2), 309–318.
Loureiro, J.B.R., Silva Freire, A.P., 2011. Scaling of turbulent separating flows. Int. J. Eng. Sci. 49 (5), 397–410.
Manes, C., Ridolfi, L., Katul, G., 2012. A phenomenological model to describe turbulent friction in permeable-wall flows. Geophys. Res. Lett. 39 (14). L14403
Marusic, I., Perry, A.E., 1995. A wall-wake model for the turbulence structure of boundary layers. Part 2. Further experimental support. J. Fluid Mech. 298, 389–407.
Marxman, G., Gilbert, M., 1963. Turbulent boundary layer combustion in the hybrid rocket. Symposium (International) on Combustion. 9. Elsevier, pp. 371–383.
McDonald, H., 1969. The effect of pressure gradient on the law of the wall in turbulent flow. J. Fluid Mech. 35 (02), 311–336.
Mendoza, C., Zhou, D., 1992. Effects of porous bed on turbulent stream flow above bed. J. Hydraul. Eng. 118 (9), 1222–1240.
Mickley, H.S., Davis, R.S., 1957. Momentum Transfer for Flow Over a Flat Plate with Blowing. Technical Notes 4017. National Advisory Committee for Aeronautics.
Moffat, R.J., Kays, W.M., 1984. A review of turbulent-boundary-layer heat transfer research at Stanford, 1958–1983. In: Hartnett, J.P., Irvine, T.F. (Eds.), Advances in Heat Transfer. 16. Elsevier, pp. 241–365.
Na, Y., Moin, P., 1998. Direct numerical simulation of a separated turbulent boundary layer. J. Fluid Mech. 374, 379–405.
Newman, B.G., 1951. Some contributions to the study of the turbulent boundary-layer near separation. In: Report ACA-53. Department of Supply, Aeronautical Research Consultative Committee.
Nezu, I., 1977. Turbulent structure in open-channel flows. Kyoto University Ph.D. thesis. English translation.
Nikitin, N.V., Pavel'ev, A.A., 1998. Turbulent flow in a channel with permeable walls. Direct numerical simulation and results of three-parameter model. Fluid Dyn. 33 (6), 826–832.
Orlando, A.F., Moffat, R.J., Kays, W.M., 1974. Turbulent transport of heat and momentum in a boundary layer subject to deceleration, suction and variable wall temperature. Report HMT-17. NASA, Stanford University.
Pak, J., 1999. A study of the thermal law of the wall for separated flow caused by a backward facing step. Texas Tech University Ph.D. thesis.
Perry, A.E., Bell, J.B., Joubert, P.N., 1966. Velocity and temperature profiles in adverse pressure gradient turbulent boundary layers. J. Fluid Mech. 25 (2), 299–320.
Rubesin, M.W., 1954. An analytical estimation of the effect of transpiration cooling on the heat-transfer and skin-friction characteristics of a compressible, turbulent boundary layer. Technical Notes 3341. National Advisory Committee for Aeronautics.
Sarnecki, A.J., 1959. The Turbulent Boundary Layer on a Permeable Surface. Cambridge University Ph.D. thesis.
Schlichting, S., 1979. Boundary-Layer Theory. McGraw-Hill, New York.
da Silva, C.B., Hunt, J.C.R., Eames, I., Westerweel, J., 2014. Interfacial layers between regions of different turbulence intensity. Ann. Rev. Fluid Mech. 46, 567–590.
Silva, T.S., da Silva, C.B., 2017. The behaviour of the scalar gradient across the turbulent/non-turbulent interface in jets. Phys. Fluids 29 (8), 085106.
Silva Freire, A.P., 1988a. An asymptotic approach for shock-wave/transpired turbulent boundary layer interactions. Zeitschrift für angewandte Mathematik und Physik ZAMP 39 (4), 478–503.
Silva Freire, A.P., 1988b. An asymptotic solution for transpired incompressible turbulent boundary layers. Int. J. Heat Mass Transfer 31 (5), 1011–1021.
Silva Freire, A.P., 1988c. An extension of the transpired skin-friction equation to compressible turbulent boundary layers. Int. J. Heat Mass Transfer 31 (11), 2395–2398.
Silva Freire, A.P., Cruz, D.O.A., Pellegrini, C., 1995. Velocity and temperature distributions in compressible turbulent boundary layers with heat and mass transfer. Int. J. Heat Mass Transfer 38 (13), 2507–2515.
Simpson, R.L., 1967. The Turbulent Boundary Layer on a Porous Plate: An Experimental Study of the Fluid Dynamics with Injection and Suction. Stanford University Ph.D. thesis.
Simpson, R.L., 1983. A model for the backflow mean velocity profile. AIAA J. 21 (1), 142–143.
Skåre, P., Krogstad, P., 1994. A turbulent equilibrium boundary layer near separation. J. Fluid Mech. 272, 319–348.
Skote, M., Henningson, D.S., 2002. Direct numerical simulation of a separated turbulent boundary layer. J. Fluid Mech. 471, 107–136.
Skote, M., Wallin, S., 2016. Near-wall damping in model predictions of separated flows. Int. J. Comput. Fluid Dyn. 30 (3), 218–230.
Stevenson, T.N., 1963. A Law of the Wall for Turbulent Boundary Layers with Suction or Injection. Report 166. College of Aeronautics, Cranfield,England.
Stratford, B.S., 1959. The prediction of separation of the turbulent boundary layer. J. Fluid Mech. 5 (1), 1–16.
Sumitani, Y., Kasagi, N., 1995. Direct numerical simulation of turbulent transport with uniform wall injection and suction. AIAA J. 33 (7), 1220–1228.
Tennekes, H., 1964. Similarity Laws for Turbulent Boundary Layers with Suction Or Injection. Report VTH-119. Technological University Delft, Department of Aeronautical Engineering.
Torii, K., Nishiwaki, N., Hirata, M., 1966. Heat transfer and skin friction in turbulent boundary layer with mass injection. Proceedings of the Third International Heat Transfer Conference. 3. Am. Inst. Chem. Engrs New York, pp. 34–48.
Townsend, A.A., 1961. Equilibrium layers and wall turbulence. J. Fluid Mech. 11 (1), 97–120.
Trip, R., Fransson, J.H.M., 2014. Boundary layer modification by means of wall suction and the effect on the wake behind a rectangular forebody. Phys. Fluids 26 (12), 125105.
Turcotte, D.L., 1960. A sublayer theory for fluid injection into the incompressible turbulent boundary layer. J. Aerosp. Sci. 27 (9), 675–678.
Vigdorovich, I., 2016. A law of the wall for turbulent boundary layers with suction: Stevenson's formula revisited. Phys. Fluids 28 (8), 085102.
Vogel, J.C., 1984. Heat Transfer and Fluid Mechanics Measurements in the Turbulent Reattaching Flow Behind a Backward-Facing Step. Stanford University Ph.D. thesis.
Watts, K.C., 1972. The Development of Asymptotic Turbulent, Transitional, and Laminar Boundary Layers Induced by Suction. University of Waterloo Ph.D. thesis.
Whitten, D.G., 1967. The Turbulent Boundary Layer on a Porous Plate: Experimental Heat Transfer with Variable Suction, Blowing and Surface Temperature. In: Report HMT-3. Stanford University.
Wilcox, D.C., 1989. Wall matching, a rational alternative to wall functions. 27th AIAA Aerospace Sciences Meeting.
Willert, C.E., 2015. High-speed particle image velocimetry for the efficient measurement of turbulence statistics. Exp. Fluids 56 (1), 17.
Yang, J.T., Tsai, B.B., Tsai, G.L., 1994. Separated-reattaching flow over a backstep with uniform normal mass bleed. J. Fluids Eng. 116 (1), 29–35.